

Comparison of three-phase reactor performances with and without packing elements

M.R. Rönnholm*, J. Wärnå, T. Salmi

Process Chemistry Group, Laboratory of Industrial Chemistry, Åbo Akademi University, FIN-20500 Åbo, Finland

Abstract

An interesting technology to carry out slow reactions with small catalyst particles is the use of static packing elements, where the solid catalyst particles are placed inside a metal network in a bubble column. The static element acts as a static mixer and ensures a low pressure drop in spite of small particle sizes. The present work concerns the mathematical modelling of bubble columns with static packing elements. Exothermic simultaneous homogeneous and heterogeneous oxidation of ferrous sulfate was chosen as a three-phase model system.

© 2003 Elsevier Science B.V. All rights reserved.

Keywords: Three-phase reactor; Packing elements; Oxidation

1. Introduction

The classical chemical approach concerns intrinsic reaction kinetics over finely dispersed catalyst particles (on a micrometer scale). The use of small particles suppresses the diffusion resistance inside the catalyst particles. The classical systems engineering approach aims at reactor models, which predict the output of the reactor equipment, i.e. the molar flows of the components. Large catalyst particles (on mm–cm scale) are often used in reactors of industrial scale, for example, in fixed bed reactors. The diffusional effects in catalyst particles are lumped together with intrinsic kinetics to ‘pseudo-kinetic’ models, which can easily be included in process simulators. These kind of ‘pseudo-kinetic’ models are, however, limited to the actual particle size: the model parameters always have to be re-estimated,

whenever the particle size is changed. In this paper, we present an approach, which is based on the intrinsic phenomena in catalyst pellets and catalytic reactors.

2. Coupled homogeneous and heterogeneous reactions

Noncatalytic and homogeneously catalyzed gas–liquid reactions take place in the liquid phase, where the gaseous reactants are absorbed and react with other reactants, which exist primarily in the liquid phase. If the reaction is instantaneous, it can take place in the liquid film around the gas bubble, and one can use a low liquid volume in relation to the volume of the diffusion layer. In the case of the oxidation of ferrous sulfate, the mass transfer of oxygen as such is not a limiting factor—since the reaction itself is the limiting factor—and so the enhancement factor is close to 1 at the reactor inlet, where the concentration of ferrous sulfate is highest (I).

* Corresponding author. Tel.: +358-2-2154431;
fax: +358-2-2154479.
E-mail address: mats.ronnholm@abo.fi (M.R. Rönnholm).

Nomenclature

| | |
|-----------|---|
| a | shape factor for catalyst particle |
| a_v | mass transfer area/volume |
| a'_v | mass transfer area/volume in metal network |
| c | concentration |
| c_L | total concentration of liquid |
| D | diffusion coefficient |
| D_e | effective diffusion coefficient |
| D_G | dispersion coefficient for gas phase |
| D_L | dispersion coefficient for liquid phase |
| D'_L | dispersion coefficient for liquid inside the metal network |
| E/R | activation energy/gas constant |
| k_G | mass transfer coefficient for gas phase |
| k_L | mass transfer coefficient for liquid phase |
| k_{Ls} | mass transfer coefficient for liquid–solid |
| m_{cat} | mass of catalyst |
| N_p | flux inside the catalyst |
| N^b | flux between the gas and liquid phase |
| N' | flux through metal network |
| r | catalytic reaction or generation rate |
| r' | noncatalytic reaction or generation rate |
| R | molar gas constant, $8.314 \text{ J mol}^{-1} \text{ K}^{-1}$ |
| R_p | catalyst particle radius |
| t | time |
| T | temperature |
| V | volume |
| w | superficial flow velocity |

Greek letters

| | |
|------------------|--|
| α | model switch |
| ε | hold-up |
| ε'_p | particle porosity |
| ε' | hold-up (metal network) |
| ρ_B | catalyst bulk density |
| ρ_P | apparent density of dry catalyst particles |
| τ_P | particle tortuosity |

Subscripts and superscripts

| | |
|----------|---------------------------|
| b | bulk |
| G | gas phase |
| L | liquid phase |
| P | particle |
| ' | properties inside network |

3. Pseudo-homogeneous and heterogeneous models for three-phase batch reactors

The models for batchwise operating stirred tank reactors were based on the following fundamental assumptions:

- The reactors operate under nonsteady state conditions and three-phases are present: a gas, a liquid and a solid catalyst phase.
- The mass transfer resistance is assumed to be located in three positions in the reactor: in the gas and liquid films at the gas–liquid interface, in the liquid film at the liquid–catalyst interface and inside the catalyst particles. Thus the model is primarily applicable for porous catalyst particles and finely suspended particles.

The well-mixed (semi-) batchwise operating slurry reactor has simple hydrodynamics, i.e. complete backmixing, which implies that no local concentration gradients appear in the bulk phases of gas and liquid. The gas phase pressure is usually controlled in the batch reactor, which implies that the mass balance equations for the gas phase are omitted. Gas–liquid reactions can, in principle, proceed in the liquid film at the gas–liquid interphase, but for moderately slow reactions the Hatta number is low, and only diffusion in the liquid phase is included in the model [1,2].

Based on these hypotheses, the liquid phase mass balance for an arbitrary component can be written as

$$\frac{dc_{Li}}{dt} = (N_{P,i}a_P)_{cat} + (N_{P,i}a_P)_{noncat} + r_{i,noncat} + k_{Li}a(c_{Li}^* - c_{Li}) \quad (1)$$

where $r_{i,noncat}$ denotes the noncatalytic generation rate. For nonvolatile compounds, $k_{Li} = 0$.

If the diffusion resistance in the catalyst particles is not accounted for, we get $N_{Pi}a_P = \rho_B r_i$, where the bulk density of the catalyst is defined as $\rho_B = m_{cat}/V_L$, and m_{cat} is the mass of the catalyst. Usually a total balance comprising both the liquid bulk and the catalyst pores is used for this case:

$$\frac{dc_{Li}}{dt} = \rho_B r_{i,cat} + r_{i,noncat} + k_{Li}a(c_{Li}^* - c_{Li}) \quad (2)$$

4. Modelling principles

Column reactors with static packing elements provide an attractive alternative for conventional reactors, since they combine the benefits of classical, fixed beds and slurry reactors: static mixing elements guarantee a good local turbulence, catalyst separation is avoided and small catalyst particles can be used. A detailed description of the reactor equipped with packing elements is provided. The modelling of the column reactor is based on verified hypotheses concerning the hydrodynamics and mass transfer conditions. The following fundamental assumptions were applied on the mathematical modelling of the reactor:

- The model is completely dynamic, accounting for the accumulation of the mass in the bulk phases of gas and liquid, as well as in the pores of the catalyst particles. Our previous experience has convincingly shown that dynamic (or pseudo-dynamic) models should be preferred not only for the prediction of transient operation periods, but also to ensure an improved robustness in the numerical solution of the model equations, particularly for counter-current operation.
- The liquid phase is distributed in the pores of the catalyst as well as inside and outside the packing network. Gas bubbles exist exclusively outside the packing network, since the bubbles are not able to penetrate through the network, the size of which is only 0.5 mm. This assumption was confirmed by visual observation of the experimental device.
- The gas and liquid flow patterns are described using the axial dispersion concept combined with plug flow. Different liquid velocities prevail inside and outside the network according to CFD calculations. Mass transfer and convection take place through the network via molecular diffusion and turbulence. Radial dispersion effects in the liquid phase were neglected in the present treatment.
- Mass transfer in the catalyst pores is described by a reaction-diffusion model, whereas an effective transport coefficient approach is applied to the flow and mass transfer between the liquid phases existing inside and outside the packing network.
- Both catalytic and noncatalytic reactions proceed simultaneously inside the wetted catalyst pores. This is particularly important for the actual application,

ferrous sulfate oxidation, where both kinds of processes are relevant.

- Isothermal cases are modelled, and therefore energy balance considerations are omitted.

5. Mass balances for bulk phases

Based on the hypotheses presented above, the mass balances can be written as follows.

Liquid phase outside the packing network:

$$\frac{dc_{Li}}{dt} = \frac{1}{\varepsilon_L} \left(-w_L \frac{dc_{Li}}{dl} + \varepsilon_L D_L \frac{d^2 c_{Li}}{dl^2} + N_{Li}^b a_v - N'_{Li} a'_v + \varepsilon_L r_{i, \text{noncat}} \right) \quad (3)$$

where $N_{Li} a_v$ denotes the diffusion flux from the gas bubbles to the liquid bulk, and $N'_{Li} a'_v$ denotes the transport from the liquid bulk into the network, which consists principally of two contributions: molecular diffusion and turbulent exchange between the material inside and outside the network. The symbols are defined in the notation.

Gas phase outside the packing network:

$$\frac{dc_{Gi}}{dt} = \frac{1}{\varepsilon_G} \left[\pm \left(\frac{dc_{Gi}}{dl} w_G + \alpha_1 \frac{dw_G}{dl} c_{Gi} \right) - \alpha_2 c_{Gi} \frac{d\varepsilon_G}{dt} + \varepsilon_G D_G \frac{d^2 c_{Gi}}{dl^2} - N_{Li}^b a_v \right] \quad (4)$$

where $\alpha_1 = 0$ or 1 and $\alpha_2 = 0$ or 1; $\alpha_1 = \alpha_2 = 1$ for cases where it is necessary to account for changes in the volumetric flow rate and hold-up of the gas; for instance, in cases where the gas phase is consumed due to the reaction. Typically, the dispersion coefficient in the gas phase (D_G) is low, and the system approaches plug flow. In Eq. (4), $-$ and $+$ signs are assigned to co-current and counter-current flows, respectively.

Inside the packing network, only the liquid phase is present, and the balance becomes

$$\frac{dc'_{Li}}{dt} = \frac{1}{\varepsilon'_L} \left(-w'_L \frac{dc'_{Li}}{dl} + \varepsilon'_L D'_L \frac{d^2 c'_{Li}}{dl^2} + N_{pL} a_p + N'_{Li} a'_v + \varepsilon' r_{\text{noncat}, i} \right) \quad (5)$$

For the reactor inlet and outlet, the boundary conditions of Danckwerts [3] are applied.

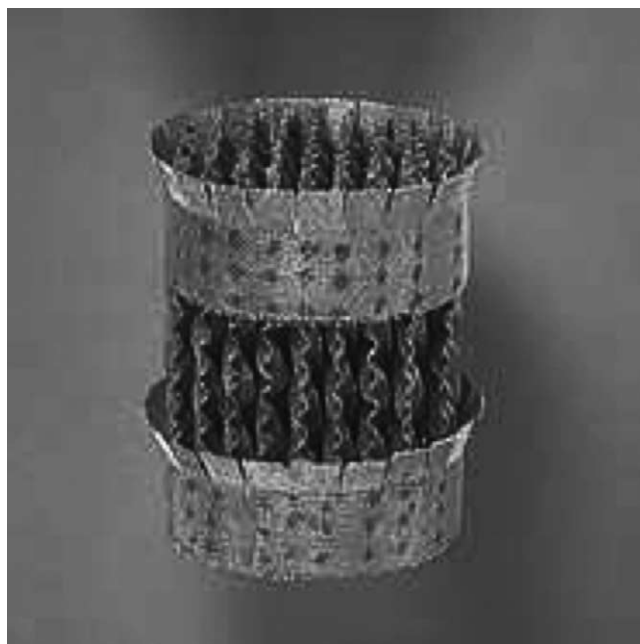


Fig. 1. Katapak S elements are bags, where wire gauze is used for holding the small catalyst particles. The small particles give a higher effectiveness factor without the problems related to slurry or packed bed reactors.

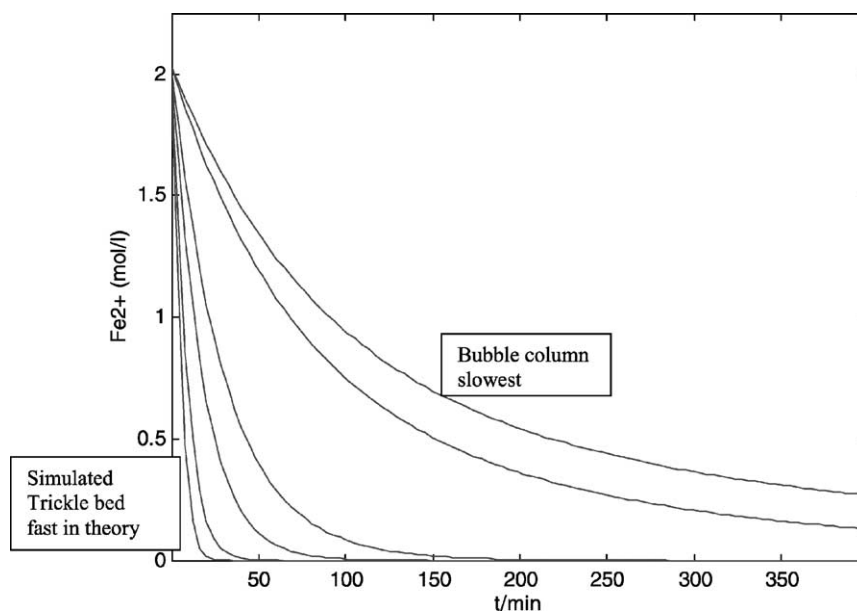


Fig. 2. Simulated results at oxygen pressure 4 bar and 333 K when using noncatalytic bubble column (slowest) and using different catalyst amounts in packing elements (Katapak options 7.1, 71, 142 kg catalyst/m³ and simulated 305 kg catalyst/m³) and finally simulated trickle bed (fastest, 710 kg catalyst/m³).

6. Application: oxidation of ferrous sulfate to ferric sulfate

The modelling concept described in previous chapters was applied on a case study: the liquid phase oxidation of ferrous sulfate to ferric sulfate. Ferric sulfate is widely used as a water purification agent,

since it has good coagulation properties. The oxidation takes place in acidic environment, in the presence of sulfuric acid. The overall reaction is shown below:

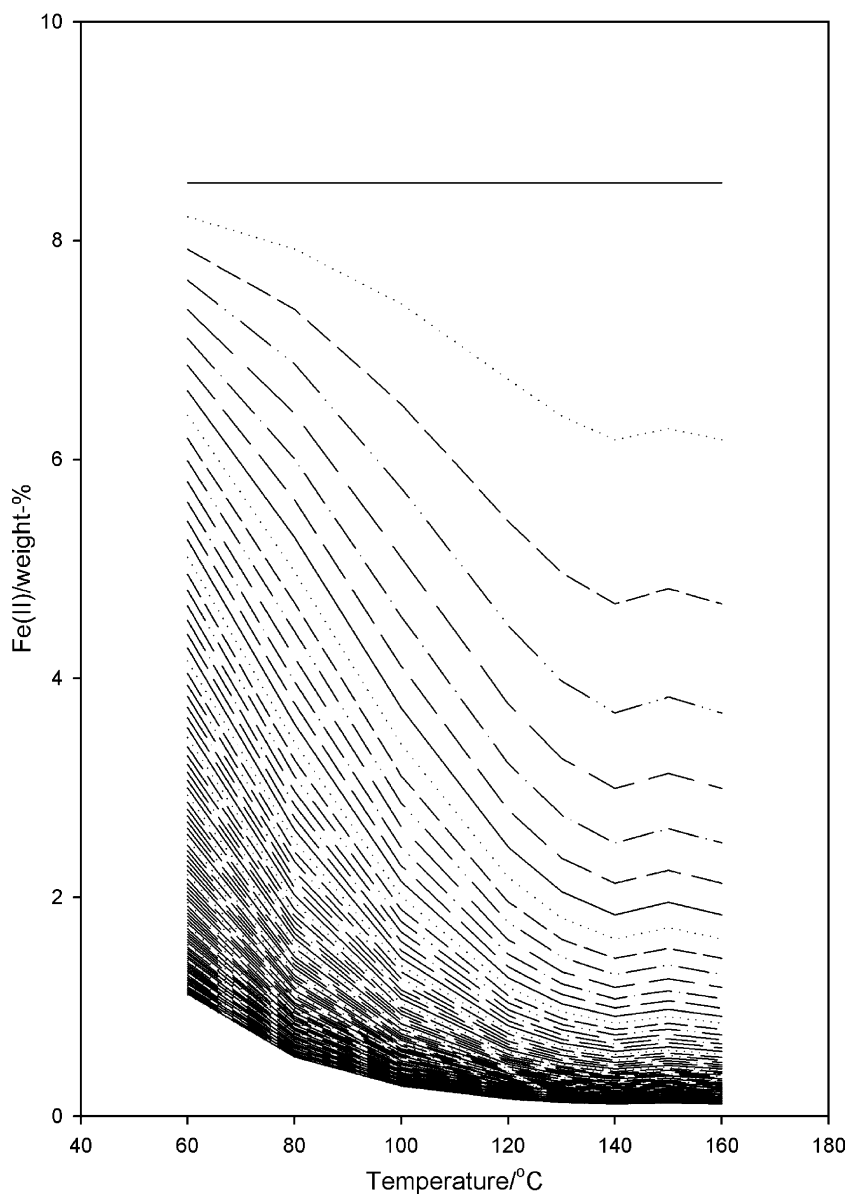
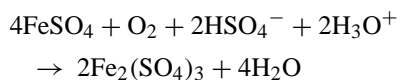


Fig. 3. Kinetics of ferrous sulfate with molecular oxygen at 4 bar. Concentration at equal time at different temperatures starting with 8.53 wt.% at 0 min ending at 97 min.

The oxidation process takes place spontaneously in liquid phase, if dissolved oxygen or air is present (nuncatalytic oxidation) [1], but the oxidation rate is enhanced by addition of a catalyst, e.g. active carbon (catalytic oxidation), that is packed in Katapak S (Fig. 1) [2,4].

7. Comparison of reactor technologies

The performance of alternative reactor technologies such as batch, continuous slurry and packed bed can also be simulated as well as different side reactor alternatives added to the existing equipment. The intensification of the process can be achieved through the well-known kinetic model and diffusion models [5–7]. The comparison of reactor technologies shown in the figures are for the sake of clarity all assumed at liquid hold-up 0.77, a catalyst diameter 1 mm, starting with Fe^{2+} equal to 2 kmol/m^3 . Further, using a temperature and catalyst with a reaction rate slow enough to allow oxygen to be available everywhere, even in the simulated trickle bed case.

The effect of adding catalyst per volume from 0 to 710 g/l is shown in Fig. 2. It clearly demonstrates the time saved at oxygen pressure 4 bar and 333 K when using a nuncatalytic bubble column (slowest) and using different catalyst amounts in slurry or packing elements (7.1 , $71 \text{ kg catalyst/m}^3$, the typical pilot $142 \text{ kg catalyst/m}^3$ and simulated $305 \text{ kg catalyst/m}^3$) and finally simulated trickle bed (fastest, $710 \text{ kg catalyst/m}^3$), with the assumption that oxygen is available everywhere. The effect of different temperatures on the homogeneous oxidation is shown in Fig. 3, here visualized in a system where we have no temperature gradient and therefore no radial dispersion. The overall oxidation order seems to be second order with respect to temperature up to 413 K. A run with the pilot reactor can be seen in Fig. 4, the model performs well.

This implies that a continuous feed at 333 K to the reactor working at the temperature about 400 K would benefit from an exothermic reaction. Packing elements could be used for start-ups with a feed at a temperature around 333 K and after a continuous reactor to reach the final low concentration.

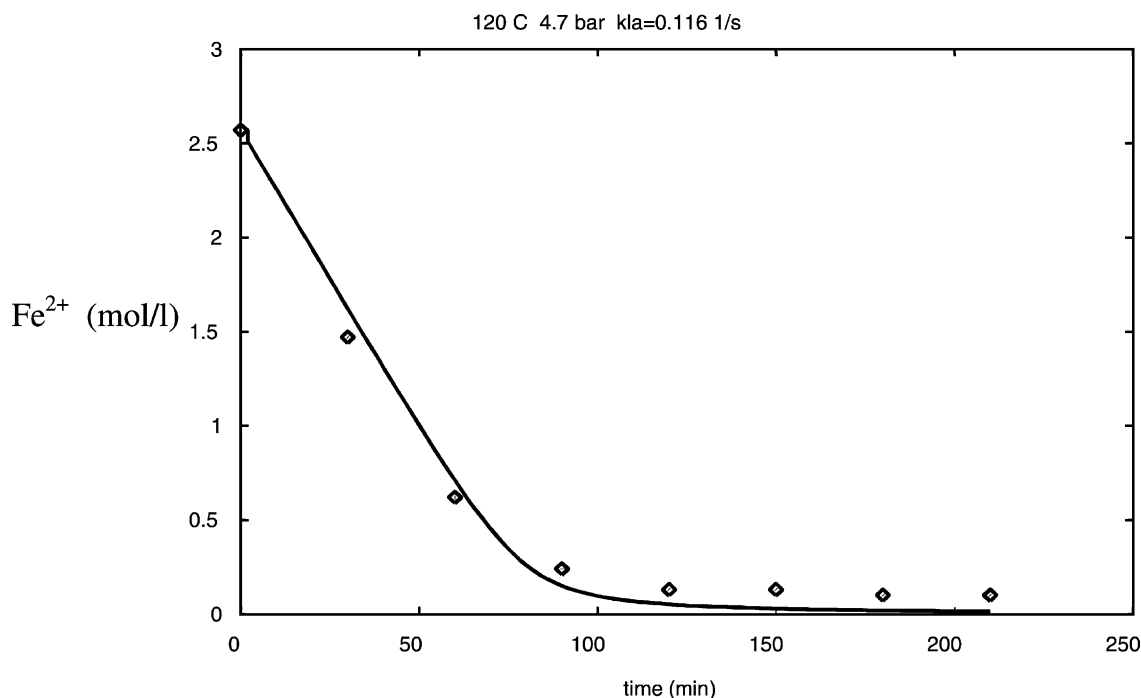


Fig. 4. Concentration of Fe^{2+} in a recirculating system with a Katapak reactor element. Experimental points and simulated lines.

8. Conclusions

A dynamic mathematical model for the three-phase reactor system with catalyst particles in static elements was derived. The model solution procedure turned out to be robust and reliable, which was illustrated with example simulations (Figs. 2 and 3). The model was verified using a realistic test system, oxidation of ferrous sulfate to ferric sulfate. The test system is relevant in the production of ferric sulfate, an efficient coagulation agent used in water purification.

The modelling concept proposed in the present work is a general one: it can be applied to any experimental system in column reactors with structured packing elements, typically for catalytic and noncatalytic hydrogenation and oxidation processes.

Acknowledgements

Financial support from Technology Development Centre (TEKES) and Kemira Research Centre (Oulu) is gratefully acknowledged. This work is part of the

activities at the Process Chemistry Group, Åbo Akademi within the Finnish Centre of Excellence Programme (2000–2005) by the Academy of Finland.

References

- [1] M.R. Rönholm, J. Wärnå, T. Salmi, I. Turunen, M. Luoma, Kinetics of oxidation of ferrous sulfate with molecular oxygen, *Chem. Eng. Sci.* 54 (1999) 4223–4232.
- [2] M.R. Rönholm, J. Wärnå, T. Salmi, I. Turunen, M. Luoma, Oxidation kinetics of ferrous sulfate over active carbon, *Ind. Eng. Chem. Res.* 38 (7) (1999) 2607–2614.
- [3] P.V. Danckwerts, Continuous flow systems, *Chem. Eng. Sci.* 2 (1) (1953) 1–13.
- [4] T. Salmi, J. Wärnå, M.R. Rönholm, I. Turunen, M. Luoma, K. Keikko, W. Levering, C. von Scala, H. Haario, Dynamic modelling of catalytic column reactor with packing elements, Presented at ECCE 2, CD-ROM of full texts.
- [5] T.A. Nijhuis, M.T. Kreutzer, A.C.J. Romijn, F. Kapteijn, J.A. Moulijn, Monolithic catalysts as efficient three-phase reactors, *Chem. Eng. Sci.* 56 (3) (2001) 823–829.
- [6] M. Piironen, H. Haario, I. Turunen, Modelling of Katapak reactor for hydrogenation of anthraquinones, *Chem. Eng. Sci.* 56 (3) (2001) 859–864.
- [7] Yu. Matatov-Meytal, M. Sheintuc, Catalytic fibers and cloths, *Appl. Catal. A* 231 (1–2) (2002) 1–16.